



HAL
open science

Temperature and salinity effects on the Raman scattering cross section of the water OH-stretching vibration band in NaCl aqueous solutions from 0 to 300 °C

Xiangen Wu, Wanjun Lu, Wenjia Ou, Marie-Camille Caumon, Jean Dubessy

► **To cite this version:**

Xiangen Wu, Wanjun Lu, Wenjia Ou, Marie-Camille Caumon, Jean Dubessy. Temperature and salinity effects on the Raman scattering cross section of the water OH-stretching vibration band in NaCl aqueous solutions from 0 to 300 °C. *Journal of Raman Spectroscopy*, 2017, 48 (2), pp.314-322. 10.1002/jrs.5039 . hal-02347839

HAL Id: hal-02347839

<https://hal.science/hal-02347839>

Submitted on 5 Nov 2019

HAL is a multi-disciplinary open access archive for the deposit and dissemination of scientific research documents, whether they are published or not. The documents may come from teaching and research institutions in France or abroad, or from public or private research centers.

L'archive ouverte pluridisciplinaire **HAL**, est destinée au dépôt et à la diffusion de documents scientifiques de niveau recherche, publiés ou non, émanant des établissements d'enseignement et de recherche français ou étrangers, des laboratoires publics ou privés.

Temperature and salinity effects on the Raman scattering cross section of the water OH stretching vibration band in NaCl aqueous solutions from 0 to 300 °C

Xianguan Wu ^a, Wanjun Lu ^{b*}, Wenjia Ou ^a, Marie-Camille Caumon ^c, Jean Dubessy ^c

^a Key Laboratory of Tectonics and Petroleum Resources of Ministry of Education, Faculty of Earth Resources, China University of Geosciences, Wuhan 430074, China

^b State Key Laboratory of Geological Processes and Mineral Resources, China University of Geosciences, Wuhan 430074, China

^c Université de Lorraine, CNRS, CREGU, GeoRessources laboratory, BP 70239, F-54506 Vandœuvre-lès-Nancy, France

* Corresponding Author. Tel.: +86 18062051972; fax: +86 27 6788 3051. E-mail: luwanjuncug@126.com (Wanjun Lu)

ABSTRACT

Water is often used as an internal standard in quantitative Raman spectroscopic measurements of dissolved species in aqueous solutions containing salts at varying temperatures. However, the effects of temperature and dissolved ions on the relative differential Raman scattering cross section (RSCS) of the OH stretching vibration band of water at elevated temperatures and salinities are not well defined quantitatively. In this study, the Raman spectra of NaCl solutions with different salinity (from 0 to 5 mol NaCl/kg-H₂O) at 20 °C at atmospheric pressure and from 0 to 300 °C at 30 MPa were studied. The relative RSCS of the OH stretching vibration band of liquid water ($\sigma_{(m\text{NaCl}, T, 30 \text{ MPa})} / \sigma_{(\text{Pure water}, 20 \text{ °C}, 30 \text{ MPa})}$) as a function of temperature (T , in °C) and salinity ($m\text{NaCl}$, in mol/kg-H₂O) was established:

$$\sigma_{(m\text{NaCl}, T, 30 \text{ MPa})} / \sigma_{(\text{Pure water}, 20 \text{ °C}, 30 \text{ MPa})} = f(T, m\text{NaCl}) = a(T-20) + b$$

where $a = 0.000089 \times m\text{NaCl}^{1/2} - 0.001164$; $b = 0.0355 \times m\text{NaCl} + 1$;

The RSCS of the OH stretching vibration band of water in pseudo back-scattering geometry decreases linearly with increasing temperature, but increases with the addition of dissolved NaCl within the whole temperature range. The enhancement factor of the RSCS by dissolved NaCl increases with temperature. Such effects of temperature and salinity should be considered in quantitative Raman spectroscopic study of species concentration in aqueous solution at high temperature when using water as internal standard.

Key words: quantitative Raman spectroscopy, water, NaCl, Raman scattering cross section, temperature

INTRODUCTION

As the most abundant liquid on the earth, water plays an essential role in countless chemical reactions occurring in living and nonliving systems because of its many unique properties. The structure and dynamics of water molecules is rather complex due to the many-body and cooperative effects related to hydrogen bonds and solute solvation.^[1] Raman spectroscopy historically has been a powerful tool for studying the structural changes occurring in water caused by temperature, pressure and dissolved ions.^[2-23] Generally, breaking hydrogen bonds by increasing temperature or ion solvation results in a decrease of inter-molecular coupling of OH-stretching vibrations.^[9] Many vibrational studies of aqueous alkali

halide solutions revealed that the perturbations of the water structure are mainly caused by the halide ions, whereas the alkali cations have relatively negligible effect on the water OH Raman band shape.^[10,12,21,23-26] Moreover, neutron scattering studies^[27] and time-resolved infrared (pump-probe) studies^[28,29] indicated that perturbations of the water structure around both anions and cations are largely localized to the first hydration shell. The OH stretching region of the Raman spectrum is a complex profile of overlapping bands and there is no general consensus in the number of underlying bands and their origin inside the complex OH profile. The OH band profile of non-polarized Raman spectra of liquid water at least consists of three main components, located

at around 3260, 3450 and 3600 cm⁻¹, which indicate different types of hydrogen bonding: multiple bond, single bond and non-bond, respectively.^[30]

Apart from application of Raman spectroscopy to molecular interactions, quantitative analytical application of Raman spectroscopy has been developed successfully in both laboratory and submarine environment at various temperature-salinity-pressure conditions because of its non-destructive and non-contact advantages. Indeed, the water stretching Raman band is often used as internal standard in the determination of aqueous dissolved species concentration in the molality scale.^[24,31-43] In our previous works, Ou et al.^[39,40] found that the Raman peak area ratio (PAR= $A_{\text{CH}_4}/A_{\text{H}_2\text{O}}$) between the stretching bands of methane and water were affected by temperature and salinity, and the effect of dissolved NaCl on the PAR/mCH₄ (mCH₄ the concentration of CH₄ by mol/kg-H₂O) became more and more significant with increasing temperature. Nevertheless, the mechanism of the dependence of PAR/mCH₄ on temperature and salinity remains unclear.

The area A of a Raman peak over a finite range of wavenumbers ($\bar{\nu}_1$ to $\bar{\nu}_2$) can be given by (modified from Wopenka and Pasteris^[44]):

$$A \propto \int_{\bar{\nu}_1}^{\bar{\nu}_2} I_{\bar{\nu}_0} \sigma_i \eta \rho \Omega d\bar{\nu} = \int_{\bar{\nu}_1}^{\bar{\nu}_2} I_{\bar{\nu}_0} \sigma_i \frac{w_i}{M_i} \rho \Omega d\bar{\nu} \quad (1)$$

Where $I_{\bar{\nu}_0}$ is the laser irradiance onto the sample, σ_i the relative differential Raman Scattering Cross Section of species i (which is a measure of the scattering efficiency of a particular vibrational mode of one molecule for given experimental geometry and polarization), η the molar density (mol.cm⁻³), w_i the mass fraction of species i in the solution, M_i the molar mass, ρ the mass density of the solution (g.cm⁻³), and Ω the solid angle of collection of the scattered Raman radiations. For two or more species in the same phase of a fluid system, the irradiance and the solid angle of collection of light are the same for all species.^[44] Obviously the dependence of the RSCS of the OH stretching vibration band of water on the temperature and dissolved ions is essential for quantifying the effect of temperature and salinity on the PAR/mCH₄ when choosing water as internal standard.

Many researchers have attempted to quantify the effect of temperature and dissolved ions on the intensity of the

OH stretching vibration band of water since 1960s.^[9,15,16,18,19,21] Although having similar effect on the Raman band profile of the OH-stretching vibrations, the increase of temperature and the addition of dissolved halide alkali/calc-alkali salts lead to contrary changes of the intensity of the OH stretching vibration band of water. The intensity of the OH stretching vibration band of water decreases with increasing temperature,^[9,16,18] but increases with the presence of dissolved halide alkali/calc-alkali salts.^[8,45,46] The band shape and the intensity of the OH stretching band are significantly affected by the intermolecular coupling^[47] and Fermi resonance (FR).^[8,9,48] Both Raman experiments^[12,49] and quantum calculations^[50,51] of ion-water clusters indicate that the RSCS of hydration water can be significantly modified by anions, but is little affected by alkali cations.^[23] A study by Raman spectroscopy of 1 M KX_(aq) solutions (X= F⁻, Cl⁻, Br⁻ and I⁻) combined with multivariate Raman curve resolution indicates that the Raman cross section (relative to bulk water) of hydration shell water molecules around F⁻, Cl⁻, Br⁻ and I⁻ is multiplied by a factor of 0.70 ± 0.1 , 1.54 ± 0.26 , 1.63 ± 0.27 , and 1.83 ± 0.32 .^[8] The charge transfer from Cl⁻, Br⁻ and I⁻ ions to the hydrating water also leads to the enhancement of the intensity of the OH stretching band of water.^[45,46] However, Wu et al.^[51] argues that the polarization effect is responsible for the increased Raman cross section of water in the presence of anions (F⁻, Cl⁻, Br⁻ and I⁻), and that the hypothesis of charge transfer is not valid to explain the Raman intensity variation.

Although numerous studies have been dedicated to the effect of dissolved ions on the RSCS of OH stretching vibration band of water, the experimental conditions were mostly limited to ambient condition. In this study, the quantitative temperature and NaCl dependence of the relative RSCS of OH stretching vibration band of water in a wide temperature range from 0 to 300 °C at 30 MPa was established for the first time. The new relative RSCS of OH stretching vibration band of water was then used to quantify the dependence on temperature and NaCl concentration of PAR/mCH₄ in the NaCl-CH₄-H₂O system.

EXPERIMENTAL

Materials

Water was ultrapurified in the laboratory with resistivity of 18.24 MΩ.cm. Aqueous solutions of different NaCl concentrations (0, 1, 2, 3 and 5 mol/kg-H₂O) were

prepared. All the reagents were analytical grade without further purification.

Apparatus and sample preparation procedures

The capillary High-Pressure Optical Cell was used in this study (Fig. 1).^[38] Experiments were conducted at ambient condition (20 °C and atmospheric pressure) and in a broad range of temperatures (0 to 300 °C) at 30 MPa.

For the ambient condition experiment, the capillary optical cell (with two open ends) was fixed on a Linkam CAP500 heating-cooling stage to ensure the same position of the laser focus for all analyses. For collecting Raman Spectra, NaCl solutions with different concentrations were injected into the capillary optical cell one by one with a syringe externally linked to one end of the capillary cell (Fig. 1a). After the measurement of a sample, the capillary optical cell must be evacuated by an empty syringe and then washed at least three times by the next sample before its spectra were collected.

For the experiment at temperatures from 0 to 300 °C at 30 MPa, round cross-sectional flexible fused silica capillary tube was used. The sample preparation procedures were similar to those described in our previous studies,^[36,40] including the following steps: (1) load an aqueous solution column (15 mm long) into a large capillary tube (665 μm OD and 300 μm ID for pressure less than or equal to 50 MPa) with one end closed; (2) insert a small tube (200 μm OD and 75 μm ID) to a certain length (10 mm) away from the end of the large tube to inject a mercury column (approximately 5 mm in length) into the aqueous solution. (3) The capillary high-pressure optical cell containing a NaCl solution at a specific concentration was connected to a high pressure line (Fig. 1b) and fixed at the experiment table to ensure that the capillary optical cell does not move during measurements at different temperatures. The pressure in the cell was maintained by water in the line and adjusted by a pressure generator, and read from a Seta 204D digital pressure transducer equipped with a Datum 2000TM manometer (69 MPa full scale; accurate to 0.14%). The temperature of the solution in the cell was maintained by a Linkam CAP500 heating-cooling stage with an accuracy of ± 0.3 K.

Spectra collection and analysis

Spectra were acquired using a JY/Horiba LabRam HR800 Raman system equipped with a frequency

doubled Nd:YAG laser (532.06 nm). The output laser power is 14 mW. The pseudo back-scattering geometry of the experiments is defined in the following way: the laser excitation and Raman scattered radiations are respectively focused and collected with a 50 X long working distance Olympus objective with a 0.5 N.A. A 300 grooves.mm⁻¹ grating together with the 800 mm focal distance of the spectrometer give a spectral resolution around 3 cm⁻¹.

Spectra were collected in the range of ~1200-4000 cm⁻¹, with the same acquisition time (80 s) and 3 accumulations. For a given experimental conditions (NaCl concentration and temperature), the focal position was always optimized to get the highest signal-to-noise ratio and kept the same for the whole spectra collection. Two or three spectra were collected for each experimental condition. The peak positions and peak area of the OH stretching vibration band of water were determined using software GRAMS/AI (Thermo Galactic).

Determination of the relative RSCS of the OH stretching vibration band of water

The relative RSCS of the OH stretching vibration band of water corresponding to this pseudo backscattering geometry were determined from the ratio between the peak area of the OH stretching bands of water. All the measured peak area should be normalized because Eq. (1) contains factors other than σ which are specific and constant for our experimental conditions. The parameters such as the laser irradiance of the specimen and the complex geometry of the Raman radiations collection in the case of cylindrical capillary can be canceled after normalization. The molar density of the sample are temperature and salinity-dependent. So the measured peak area was corrected by the molar density of the solution. η was calculated from the ρ based on the model of Mao and Duan^[52] by the factor w_i/M_i from equation 1. The relative RSCS of the water OH stretching vibration band of NaCl solutions at ambient conditions were determined by the following equation referencing to the pure water signal at 20 °C at atmospheric pressure:

$$\frac{\sigma_{OH(mNaCl, 20^\circ C, Atm)}}{\sigma_{OH(Pure\ water, 20^\circ C, Atm)}} = \frac{A_{(mNaCl, 20^\circ C, Atm)}}{\eta_{(mNaCl, 20^\circ C, Atm)}} / \frac{A_{(Pure\ water, 20^\circ C, Atm)}}{\eta_{(Pure\ water, 20^\circ C, Atm)}} \quad (2)$$

where $mNaCl$ is the concentration of NaCl (mol/kg·H₂O), Atm referred to atmospheric pressure, and $A_{(mNaCl, 20^\circ C, Atm)}$ the peak area of the OH stretching vibration band of water

in a solution at a $m\text{NaCl}$ concentration at 20 °C at atmospheric pressure.

The spectra at pressure from 0.1 to 30 MPa at 20 °C revealed that the pressure dependence is negligible within our pressure range (less than 1% difference for the peak area of OH stretching band of water at 0.1 and 30 MPa). All the spectra collected at 30 MPa are normalized by an intensity correction factor, β :

$$\beta_{(m\text{NaCl}, T, 30\text{MPa})} = \frac{\sigma_{\text{OH}(m\text{NaCl}, 20^\circ\text{C}, \text{Atm})}}{\sigma_{\text{OH}(\text{Pure water}, 20^\circ\text{C}, \text{Atm})}} \times \frac{A_{(\text{Pure water}, 20^\circ\text{C}, 30\text{MPa})}}{\eta_{(\text{Pure water}, 20^\circ\text{C}, 30\text{MPa})}} / \frac{A_{(m\text{NaCl}, 20^\circ\text{C}, 30\text{MPa})}}{\eta_{(m\text{NaCl}, 20^\circ\text{C}, 30\text{MPa})}} \quad (3)$$

So the relative RSCS of the OH stretching vibration band of water at temperature from 0 to 300 °C at 30 MPa can be calculated by the following equation, and the condition $T = 20$ °C at 30 MPa for pure water was chosen as a reference in this study:

$$\frac{\sigma_{\text{OH}(m\text{NaCl}, T, 30\text{MPa})}}{\sigma_{\text{OH}(\text{Pure water}, 20^\circ\text{C}, 30\text{MPa})}} = \beta \times \left(\frac{A_{(m\text{NaCl}, T, 30\text{MPa})}}{\eta_{(m\text{NaCl}, T, 30\text{MPa})}} / \frac{A_{(\text{Pure water}, 20^\circ\text{C}, 30\text{MPa})}}{\eta_{(\text{Pure water}, 20^\circ\text{C}, 30\text{MPa})}} \right) \quad (4)$$

RESULTS

The effect of dissolved NaCl on the relative RSCS of the OH stretching vibration band of water at 20 °C at atmospheric pressure

Figure 2 displays the molar density-corrected spectra of the OH stretching vibration band of water for different NaCl solutions at 20 °C at atmospheric pressure. With increasing concentration of NaCl, the intensity of the shoulder around 3260 cm^{-1} decreases, the intensity of the main peak around 3450 cm^{-1} increases. Dissolved NaCl reduces the width of the OH stretching band and causes the band position shift toward higher Raman shift wavenumbers. This change in the band shape is similar to the effect of increasing temperature on the Raman spectra of water.^[9,16,53]

It is obvious that the decrease in intensity of the shoulder at around 3260 cm^{-1} (strongly H-bonded water OH oscillator) is significantly weaker than the increase of the main peak at around 3450 cm^{-1} (less strongly H-bonded water OH oscillator). It leads to an increase of the overall area of the OH stretching vibration band of water with the concentration of NaCl. Table 1 is the measured peak area and the determined relative RSCS of OH stretching vibration band of water based on the reference condition for pure water at 20 °C at atmospheric pressure ($\sigma_{(m\text{NaCl}, 20^\circ\text{C}, \text{Atm})}/\sigma_{(\text{Pure water}, 20^\circ\text{C}, \text{Atm})}$). $\sigma_{(m\text{NaCl}, 20^\circ\text{C}, \text{Atm})}/\sigma_{(\text{Pure water}, 20^\circ\text{C}, \text{Atm})}$ increased linearly with the concentration of NaCl ($m\text{NaCl}$, mol/kg- H_2O):

$$\sigma_{(m\text{NaCl}, 20^\circ\text{C}, \text{Atm})}/\sigma_{(\text{Pure water}, 20^\circ\text{C}, \text{Atm})} = 0.0355 \times m\text{NaCl} + 1, \quad R^2 = 0.999 \quad (5)$$

The effect of temperature and dissolved NaCl on the relative RSCS of the OH stretching vibration band of water at temperature from 0 to 300 °C at 30 MPa

Figure 3 displays the molar density- and intensity-corrected spectra of the OH stretching vibration band of water for different NaCl solutions from 0 to 300 °C at 30 MPa.

Similar to the effect of dissolved NaCl under ambient condition, the position of the shoulder at around 3260 cm^{-1} remains unchanged and the intensity decreases with increasing temperature. The temperature dependence of the maximum peak above 3450 cm^{-1} is much different from that of the shoulder (Fig. 3). First of all, the position of the peak maximum shifts to higher wavenumbers with increasing temperature. Secondly, the variation of its intensity with temperature is much more complicated than that of the shoulder. Specifically, for pure water, the maximal intensity of the band remains almost unchanged up to 140 °C and then increases unambiguously with rising temperature. For the 3 m NaCl solution, the maximal intensity of the band remains almost the same within the whole temperature range. The maximal intensity of the band for the 5 m NaCl solution decreases quite slightly up to 240 °C and then increases slightly from 240 to 300 °C.

After normalization by molar density and by the intensity correction factor β , the relative RSCS of the OH stretching vibration band of water based on the reference condition $T = 20$ °C for pure water at 30 MPa ($\sigma_{(m\text{NaCl}, T, 30\text{MPa})}/\sigma_{(\text{Pure water}, 20^\circ\text{C}, 30\text{MPa})}$) is determined for this Raman scattering geometry (Fig. 4). Three conclusions can be drawn: (1) At constant NaCl concentration, the relative RSCS of the OH stretching vibration band of water decreases linearly with increasing temperature; (2) At constant temperature, the RSCS of the OH stretching vibration band of water increases with the dissolved NaCl concentration within the whole temperature range; (3) The enhancement factor of the RSCS of the OH stretching vibration band of water by dissolved NaCl increases with rising temperature. $\sigma_{(m\text{NaCl}, T, 30\text{MPa})}/\sigma_{(\text{Pure water}, 20^\circ\text{C}, 30\text{MPa})}$ can be represented as a function of temperature (T in °C) and $m\text{NaCl}$ (mol/kg- H_2O):

$$\sigma_{(m\text{NaCl}, T, 30\text{MPa})}/\sigma_{(\text{Pure water}, 20^\circ\text{C}, 30\text{MPa})} = f(T, m\text{NaCl}) = a(T - 20) + b \quad (6)$$

where $a = 0.000089 \times m\text{NaCl}^{1/2} - 0.001165$, $R^2 = 0.991$; $b = 0.0355 \times m\text{NaCl} + 0.9989$, $R^2 = 1.000$;

DISCUSSION

The effect of temperature on the relative RSCS of the OH stretching vibration band of water

As shown in Figure 3, the behavior of the spectra in all series is very similar, which is a clear indication of the significant weakening of the H-bond in all solutions with the increase of temperature.^[54] According to the Placzek theory, for freely rotating molecule, when the angle between the incident radiation and the direction of observation is 90° or 180° , the expression for the differential Raman cross section^[55] is:

$$\frac{d\sigma}{d\Omega} = \frac{(2\pi)^4 b_j^2 g_j (45\alpha_j'^2 + 7\gamma_j'^2)(\nu_o - \nu_j)^4}{45[1 - \exp(-hcv_j / kT)]} \quad (7)$$

Where b_j^2 is the zero point amplitude of the j th vibrational mode, g_j the vibrational degeneracy, α_j' the trace and γ_j' the anisotropy of the derived polarizability tensor, ν_o the wavenumber of the exciting radiation in m^{-1} , ν_j the wavenumber in m^{-1} of the vibrational mode j , and h , c , k , and T the Plank constant, the speed of light, the Boltzmann constant, and absolute temperature (K) respectively. Although the Placzek theory has been applied nearly universally, experimental data show an increase of the RSCS by a factor L from low density vapor to liquid density for which molecules are not randomly oriented and freely rotating; this intensity increase is named the internal field effect:

$$\frac{d\sigma}{d\Omega}(\text{liquid}) = \frac{d\sigma}{d\Omega}(\text{vapor}) \times L \quad (8)$$

The local field correction factor L can be given by equation (9)^[56]:

$$L = \frac{n_s(n_s + 2)^2(n_o + 2)^2}{81n_o} \approx \frac{(n_o + 2)^4}{81} \quad (9)$$

where n_s and n_o are the refractive index of the liquid sample at the wavelength of the Raman scattered radiation and at the wavelength of the exciting radiation. The internal field factor explains the increase of the Raman intensity in liquid by density effects only. The refractive indexes of liquid water at $\lambda=706.52$ nm and

$\lambda=650.84$ nm from 0 to 300°C at 30 MPa were both used to calculate L .^[57] The calculation shows that the effect of wavelength is weak, so the hypothesis $n_s=n_o$ is valid for all the wavenumber range of the profile of the OH stretching vibration. Consequently, in the absence of other processes, a decrease of density resulting from the increase of temperature at constant pressure should result in a decrease in intensity by the same factor for all the OH oscillators at the origin of the profile. The extent of this decrease is calculated in table 2 and is smaller than the experimental values. In addition, the field effect factor cannot account for the modification of the profile of the OH-stretching Raman band.

The statistical factor S , expressed by $(1 - \exp(-hcv/kT))^{-1}$, contains two parameters, the wavenumber of the vibration and temperature. First, this equation shows that the statistical factor is increasing with temperature for a given wavenumber value. Table 2 shows this variation is completely negligible in the range $20\text{-}300^\circ\text{C}$ (less than 0.0001%). In addition, the effect of the wavenumber is also insignificant (the difference for the relative S is less than 0.08% when the wavenumber ranges from 2800 to 3700 cm^{-1}).

Therefore, the local field factor can only explain partially the variation of the RSCS of the OH-stretching vibration and of the band profile for pure water at 300°C . It is reasonable to consider that this temperature effect in pure water solutions also applies to NaCl-bearing aqueous solutions.

According to equation (7) the RSCS also depends on the derivatives of the polarizability tensor invariants, $a_j'^2$ and $\gamma_j'^2$. The quantity $g(45a_j'^2 + 7\gamma_j'^2)$, referred to as the scattering activity, was found to be phase independent in most cases, except for the hydrogen bonded liquids.^[55,58] Rull and de Saja^[11] studied the isotropic and anisotropic components of the OH stretching band as a function of solute concentration (types AB and AB₂, A=Li, Na, K, Ca; B=Cl, Br, I, NO₃) and temperature. They found that the isotropic part $45a_j'^2$ does not vary with the concentration of NaCl but the anisotropic part $3\gamma_j'^2$ increases with NaCl concentration. Based on previous studies,^[9,59,60] Rull and de Saja concluded that both the isotropic and anisotropic parts decrease with temperature. Abe and Ito^[45] studied the effect of hydrogen bonding on the Raman intensity of methanol, ethanol and water. They attributed the observed intensity enhancement of the OH stretching band when changing from gas to liquid to the additional

contribution of the charge transfer electronic excited state arising from hydrogen bond formation. But so far it is still impossible to calculate from ab initio models to what extent the degree of hydrogen bonding in the system affects the Raman intensity of the stretching band and its profile. Intra- and inter-molecular interaction and FR due to the hydrogen bond make it much more complex.

The effect of dissolved NaCl on the relative RSCS of the water OH stretching vibration band at different temperatures

The increase of the RSCS of the OH-stretching vibration band of water with salt concentration at ambient conditions was evidenced in many studies [8,12,23,46] and is confirmed in this study. The anisotropic environment of water molecules in an aqueous electrolyte is likely to reduce the intermolecular coupling and FR, which in turn would alter the RSCS of water.[61,62] Moreover, the RSCS of the OH-stretching vibration band of water increases with the size of the halide ions.[8,46] Mondal et al.[46] attribute the increased Raman intensity of water to the charge transfer from the halide ions to the combined anti-bonding orbitals of hydrating water. However, the study from Wu et al.[51] indicates that it is the polarization effect that makes the main contribution.

The influence of dissolved NaCl on the RSCS of the OH-stretching vibration band of water at high temperature is also revealed in this study (Fig. 4). Figure 4 shows that the amplitude of the enhancement of the RSCS of water by dissolved NaCl increases with temperature. The RSCS (relative to pure water) of the OH stretching vibration band of water for 1 m, 2 m, 3 m, 5 m NaCl solutions were 1.04, 1.07, 1.11 and 1.18 at 20 °C and then increase to 1.08, 1.13, 1.21 and 1.34 at 300 °C, respectively.

The molar density- and intensity-corrected Raman spectra of NaCl aqueous solutions with various NaCl concentrations at different temperatures may provide some important information for this phenomena (Fig. 5). In spite of the extent of the ionic perturbation to the local structure still being controversial, the impact of ions on the water structure due to the interaction between the Na⁺ and Cl⁻ and water molecules in the ionic hydration shells has been confirmed by many studies.[63-66] However, Na⁺ has only a negligible effect on the OH stretching vibration band of water and the spectral change of the water OH stretching vibration band of water was mainly attributed

to the perturbation of water molecules in the hydration shell of Cl⁻. [10,12,21,23] As shown in Figure 5, at temperature below 160 °C, the intensity of the shoulder around 3260 cm⁻¹ decreases with the addition of NaCl. That of the intensity maximum around 3450 cm⁻¹ increases and slightly shifts towards higher wavenumbers. These variations are usually attributed to the conversion of strong H-bonded water to weakly H-bonded water by dissolved NaCl.[46] When the temperature increases at around 160 °C the position of the shoulder and main peak almost both remains the same with the addition of NaCl. Then, a reverse trend occurs at temperatures above 160 °C (300 °C is selected for an example): with the addition of NaCl, the intensity of the shoulder increases obviously and that of the main peak varies little. Meanwhile, the position of the main peak shifts to lower wavenumbers with increasing NaCl concentration. This reverse trend indicates that the H-bonding energy in NaCl aqueous solutions is higher than that in pure water at higher temperatures.

These observations may result from changes in dissolved ions speciation with temperature (Na⁺ and Cl⁻ solvation and NaCl^o ion pair formation), modifying the structure of water. Raising both the concentration of NaCl[65] and the temperature[67] will promote the formation of NaCl^o ion pair. So the ion-ion interactions may play an important role in determining the structure and properties of electrolyte solutions at high temperatures.[68,69] Bondarenko et al.[67] found that the number of O-H...Cl⁻ bonds decreases partially because of ion pairing at increasing temperature. So the water structure in the solutions become closer to those of pure water at high temperature, looking like a mixture of water and NaCl^o dipoles. Our result also shows that the perturbation by NaCl of the local structure of water decreases with increasing temperature. As a result, with the decreasing of the Cl⁻ concentration as a consequence of NaCl^o ion pair formation with increasing temperature, the effect of charge transfer should be weakened. This is contrary to the increase of the enhancement factor of the RSCS of water by dissolved NaCl with increasing temperature.

The implication of the variation of the RSCS of the OH stretching vibration band of water for temperature and salinity dependence of Raman quantitative factors

As an example, we have chosen the NaCl-CH₄-water system to study the effect of temperature- and salinity-

dependent RSCS of the OH stretching vibration band of water on the PAR/mCH₄ from Ou et al.^[39,40] PAR/mCH₄ can be represented by the following equation:

$$PAR / mCH_4 = (\sigma_{CH_4} / \sigma_{H_2O}) / (1000 / M_{H_2O}) \quad (10)$$

So the relative PAR/mCH₄ based on the reference condition $T = 20$ °C for pure water system (termed as PAR*/mCH₄) can be expressed by equation (11):

$$PAR^*/mCH_4 = PAR / mCH_{4(mNaCl,T)} / PAR / mCH_{4(Pure\ water,20\ ^\circ C)} = \left(\sigma_{CH_4(mNaCl,T)} / \sigma_{CH_4(Pure\ water,20\ ^\circ C)} \right) \times \left(\sigma_{H_2O(Pure\ water,20\ ^\circ C)} / \sigma_{H_2O(mNaCl,T)} \right) \quad (11)$$

It can be seen that the PAR*/mCH₄ is related to the variation of the RSCS of the symmetric stretching vibration of methane ($\sigma_{CH_4(mNaCl, 20\ ^\circ C, 30\ MPa)} / \sigma_{CH_4(mNaCl, T, 30\ MPa)}$) and the OH stretching vibration band of water ($\sigma_{H_2O(mNaCl, 20\ ^\circ C, 30\ MPa)} / \sigma_{H_2O(mNaCl, T, 30\ MPa)}$). As discussed above, the dependence of the RSCS of the OH stretching vibration band of water on pressure can be ignored within our experiment pressure condition. So the effect of temperature and dissolved NaCl on the RSCS of OH stretching vibration band of water were considered in this study. It should be noted that a new method was applied in this study to calculate the value of PAR/mCH₄ which were underestimated by Ou et al.^[39,40] resulting from the underestimation of the value of A_{CH_4} (Fig. 6). So the area difference between the spectrum of methane-bearing solution from Ou et al.^[39,40] and the spectrum of the solution without methane at the same temperature and salinity from this study were employed to calculate the A_{CH_4} . And then the new PAR/mCH₄ were obtained in this study for further comparison and discussion.

Figure 7 shows the experimental data of PAR*/mCH₄ and the $\sigma_{(mNaCl, 20\ ^\circ C, 30\ MPa)} / \sigma_{(mNaCl, T, 30\ MPa)}$ calculated by the equation (6) from this study. Apparently the variation trend of PAR*/mCH₄ is identical to that of $\sigma_{(mNaCl, 20\ ^\circ C, 30\ MPa)} / \sigma_{(mNaCl, T, 30\ MPa)}$ ratio, increasing with temperature and decreasing with the presence of NaCl. This implies that the dependence of the PAR*/mCH₄ on temperature and NaCl concentration is mainly caused by the variation of the RSCS of the OH stretching vibration band of water with increasing temperature and the addition of NaCl salts. The RSCS of the symmetric vibration band of dissolved methane is almost independent on temperature and dissolved NaCl concentration. The PAR with constant dissolved CH₄ concentration can be increased by about 47%, 34% and 29% by the decreasing RSCS of the OH stretching vibration band of water when the temperature

increased from 20 to 300 °C for pure water, 3 m NaCl and 5 m NaCl aqueous system, respectively. The decrease of the PAR with constant dissolved CH₄ concentration which results from the enhancement of RSCS of the OH stretching vibration band of water with the addition of NaCl is relatively small at low temperatures (with deviation of about 10% and 15% for 3 m NaCl and 5 m NaCl at 20 °C), and it becomes more and more significant with increasing temperature (with deviation of up to about 18% and 26% for 3 m NaCl and 5 m NaCl at 300 °C). So the dependence of the RSCS of the OH stretching vibration band of water on temperature and dissolved salts must be considered when using water as internal standards for Raman quantitative application, especially under high temperature conditions. It should also be noted that the empirical equation established by Ou et al.^[39,40] is still valuable only if the same integration method of CH₄ peak is taken with them.

SUMMARY AND CONCLUSIONS

We investigated temperature- and salinity-dependence of the RSCS of the OH stretching vibration band of water, and found it linearly decreases with increasing temperature whereas the addition of NaCl at constant temperature increases its value. The influence of dissolved NaCl on the RSCS of the OH stretching vibration band of water becomes more and more significant with rising temperature. The temperature- and salinity-dependence of the relative RSCS of the OH stretching vibration band of water mainly accounts for the dependence on temperature and salinity of the PAR/mCH₄ in CH₄ homogeneous solutions. When temperature increases from 20 to 300 °C, the RSCS of the OH stretching vibration band of water would induce about 47%, 34% and 29% error for the determined concentration of dissolved CH₄ (in mol/kg-H₂O) by Raman spectroscopy using water as internal standard for pure water, 3 m NaCl and 5 m NaCl aqueous system, respectively. The concentration error of dissolved CH₄ brought about by the addition of dissolved NaCl becomes more and more obvious with rising temperature. Equation (6) can be used to quantify such effects of temperature and NaCl concentration.

The study of the role of the derivatives of the polarizability tensor invariants, a_j^2 and γ^2 , which vary with the variation of hydrogen bonding with temperature and salt ions through molecular interactions, is essential for the

interpretation of the temperature and dissolved ions dependence of the RSCS of the OH stretching vibration band of water. The temperature- and salinity-dependences of Raman spectra of isotopically diluted water which is free from intramolecular and intermolecular coupling and FR may be promising for studying the degree of the impact of these factors on the RSCS of the OH stretching vibration band of water.

ACKNOWLEDGEMENTS

We thank Dr. I-Ming Chou and Dr. R.C. Burruss for their kind help and guidance for many years on the Raman spectroscopic research on Geo-fluids. This work was partly supported by the National Sciences Foundation of China (No. 41102154, 41176047), the Key Project of Chinese Ministry of Education (No. 109108), and the Programme of Introducing Talents of Discipline to Universities (No. B14031) by Ministry of Education. This study was also partly supported by CNRS, Université de Lorraine and ANR Program (SEED, CGS Microlab).

REFERENCES

- [1] R. Ludwig, *Angew. Chem., Int. Ed.* **2001**; *40*, 1808.
- [2] C. H. Giammanco, D. B. Wong, M. D. Fayer, *J. Phys. Chem. B* **2012**; *116*, 13781.
- [3] Q. Hu, H. Guo, W. Lu, X. Lü, Y. Chen, L. Lin, *J. Mol. Liq.* **2014**; *199*, 83.
- [4] W. Hua, D. Verreault, Z. Huang, E. M. Adams, H. C. Allen, *J. Phys. Chem. B* **2014**; *118*, 8433.
- [5] D. Jiao, C. King, A. Grossfield, T. A. Darden, P. Ren, *J. Phys. Chem. B* **2006**; *110*, 18553.
- [6] H. Kanno, J. Hiraishi, *J. Raman Spectrosc.* **1987**; *18*, 157.
- [7] R. Li, Z. Jiang, F. Chen, H. Yang, Y. Guan, *J. Mol. Struct.* **2004**; *707*, 83.
- [8] P. N. Perera, B. Browder, D. Ben-Amotz, *J. Phys. Chem. B* **2009**; *113*, 1805.
- [9] C. Ratcliffe, D. Irish, *J. Phys. Chem.* **1982**; *86*, 4897.
- [10] F. Rull, *Pure Appl. Chem.* **2002**; *74*, 1859.
- [11] F. Rull, J. De Saja, *Journal of Raman spectroscopy* **1986**; *17*, 167.
- [12] J.-W. Schultz, D. Hornig, *J. Phys. Chem.* **1961**; *65*, 2131.
- [13] Q. Sun, *Vib. Spectrosc.* **2012**; *62*, 110.
- [14] S. T. van der Post, H. J. Bakker, *Phys. Chem. Chem. Phys.* **2012**; *14*, 6280.
- [15] G. Walrafen, *J. Chem. Phys.* **1964**; *40*, 3249.
- [16] G. Walrafen, *J. Chem. Phys.* **1967**; *47*, 114.
- [17] G. Walrafen, *J. Chem. Phys.* **2004**; *120*, 4868.
- [18] G. Walrafen, M. Fisher, M. Hokmabadi, W. H. Yang, *J. Chem. Phys.* **1986**; *85*, 6970.
- [19] G. Walrafen, M. Hokmabadi, W. Yang, G. Piermarini, *J. Phys. Chem.* **1988**; *92*, 4540.
- [20] G. Walrafen, M. Hokmabadi, W. H. Yang, *J. Chem. Phys.* **1986**; *85*, 6964.
- [21] G. E. Walrafen, *J. Chem. Phys.* **1962**; *36*, 1035.
- [22] Y. Yan, X.-x. Ou, H.-p. Zhang, *J. Mol. Struct.* **2014**; *1074*, 310.
- [23] Y. Yoshimura, H. Kanno, *J. Raman Spectrosc.* **1996**; *27*, 671.
- [24] M.-C. Caumon, J. Dubessy, P. Robert, A. Tarantola, *Eur. J. Mineral.* **2013**; *25*, 755.
- [25] J. Dubessy, T. Lhomme, M.-C. Boiron, F. Rull, *Appl. Spectrosc.* **2002**; *56*, 99.
- [26] J.-J. Max, C. Chapados, *J. Phys. Chem. A* **2001**; *105*, 10681.
- [27] A. K. Soper, K. Weckström, *Biophys. Chem.* **2006**; *124*, 180.
- [28] M. Kropman, H.-K. Nienhuys, H. Bakker, *Phys. Rev. Lett.* **2002**; *88*, 077601.
- [29] M. F. Kropman, H. J. Bakker, *J. Am. Chem. Soc.* **2004**; *126*, 9135.
- [30] J. Dubessy, M.-C. Caumon, F. Rull, *Raman spectroscopy applied to earth sciences and cultural heritage*; The Mineralogical Society of Great Britain and Ireland, 2012; Vol. 12.
- [31] T. Beuvier, B. Calvignac, J.-F. o. Bardeau, A. Bulou, F. Boury, A. Gibaud, *Anal. Chem.* **2014**; *86*, 9895.
- [32] M.-C. Caumon, P. Robert, E. Laverret, A. Tarantola, A. Randi, J. Pironon, J. Dubessy, J.-P. Girard, *Chem. Geol.* **2014**; *378*, 52.
- [33] J. Chen, H. Zheng, W. Xiao, Y. Zeng, K. Weng, *Geochim. Cosmochim. Acta* **2004**; *68*, 1355.
- [34] K. Furić, I. Ciglencčki, B. Čosović, *J. Mol. Struct.* **2000**; *550*, 225.
- [35] D. Guillaume, S. Teinturier, J. Dubessy, J. Pironon, *Chem. Geol.* **2003**; *194*, 41.
- [36] H. Guo, Y. Chen, Q. Hu, W. Lu, W. Ou, L. Geng, *Fluid Phase Equilib.* **2014**; *382*, 70.
- [37] H. Lamadrid, W. Lamb, M. Santosh, R. Bodnar, *Gondwana Res.* **2014**; *26*, 301.
- [38] W. Lu, I. M. Chou, R. C. Burruss, *Geochim. Cosmochim. Acta* **2008**; *72*, 412.
- [39] W. Ou, L. Geng, W. Lu, H. Guo, K. Qu, P. Mao, *Fluid Phase Equilib.* **2015**; *391*, 18.
- [40] W. Ou, H. Guo, W. Lu, X. Wu, I.-M. Chou, *Chem. Geol.* **2015**; *417*, 1.

- [41] J. Pironon, J. O. Grimmer, S. Teinturier, D. Guillaume, J. Dubessy, *J. Geochem. Explor.* **2003**; 78, 111.
- [42] Q. Sun, C. Qin, *Chem. Geol.* **2011**; 283, 274.
- [43] Q. Sun, L. Zhao, N. Li, J. Liu, *Chem. Geol.* **2010**; 272, 55.
- [44] B. Wopenka, J. D. Pasteris, *Appl. Spectrosc.* **1986**; 40, 144.
- [45] N. Abe, M. Ito, *J. Raman Spectrosc.* **1978**; 7, 161.
- [46] M. Ahmed, A. K. Singh, J. A. Mondal, S. K. Sarkar, *J. Phys. Chem. B* **2013**; 117, 9728.
- [47] M. Yang, J. Skinner, *Phys. Chem. Chem. Phys.* **2010**; 12, 982.
- [48] J. Wiafe-Akenten, R. Bansil, *J. Chem. Phys.* **1983**; 78, 7132.
- [49] A. W. Omta, M. F. Kropman, S. Woutersen, H. J. Bakker, *Science* **2003**; 301, 347.
- [50] J. D. Smith, R. J. Saykally, P. L. Geissler, *J. Am. Chem. Soc.* **2007**; 129, 13847.
- [51] D.-Y. Wu, S. Duan, X.-M. Liu, Y.-C. Xu, Y.-X. Jiang, B. Ren, X. Xu, S. Lin, Z.-Q. Tian, *J. Phys. Chem. A* **2008**; 112, 1313.
- [52] S. Mao, Z. Duan, *J. Chem. Thermodyn.* **2008**; 40, 1046.
- [53] Q. Hu, X. Lü, W. Lu, Y. Chen, H. Liu, *J. Mol. Spectrosc.* **2013**; 292, 23.
- [54] D. Eisenberg, W. Kauzmann, *The structure and properties of water*, Oxford University Press on Demand, 2005.
- [55] J. R. Nestor, E. R. Lippincott, *J. Raman Spectrosc.* **1973**; 1, 305.
- [56] G. Eckhardt, W. G. Wagner, *J. Mol. Spectrosc.* **1966**; 19, 407.
- [57] I. Thormählen, J. Straub, U. Grigull, *J. Phys. Chem. Ref. Data* **1985**; 14, 933.
- [58] T. Fujiyama, *Bull. Chem. Soc. Jpn.* **1973**; 46, 87.
- [59] D. A. Long, *New York* **1977**, 1.
- [60] C. Luu, D. V. Luu, F. Rull, F. Sopron, *J. Mol. Struct.* **1982**; 81, 1.
- [61] H. Kanno, J. Hiraishi, *J. Phys. Chem.* **1983**; 87, 3664.
- [62] D. Hare, C. Sorensen, *J. Chem. Phys.* **1992**; 96, 13.
- [63] M. Carrillo-Tripp, H. Saint-Martin, I. Ortega-Blake, *J. Chem. Phys.* **2003**; 118, 7062.
- [64] A. Chandra, *Phys. Rev. Lett.* **2000**; 85, 768.
- [65] R. Mancinelli, A. Botti, F. Bruni, M. Ricci, A. Soper, *J. Phys. Chem. B* **2007**; 111, 13570.
- [66] R. Mancinelli, A. Botti, F. Bruni, M. Ricci, A. Soper, *Phys. Chem. Chem. Phys.* **2007**; 9, 2959.
- [67] G. Bondarenko, Y. E. Gorbaty, A. Okhulkov, A. Kalinichev, *J. Phys. Chem. A* **2006**; 110, 4042.
- [68] S. Koneshan, J. C. Rasaiah, L. X. Dang, *J. Chem. Phys.* **2001**; 114, 7544.
- [69] D. M. Sherman, M. D. Collings, *Geochem. Trans.* **2002**; 3, 1.

FIGURE CAPTIONS

Figure 1. Schematic diagram of the capillary optical cell system for collecting the Raman spectra of NaCl solutions.

Figure 2. The molar density-corrected spectra of the OH stretching vibration band of water for different NaCl solutions at 20 °C at atmospheric pressure.

Figure 3. Molar density- and intensity-normalized spectra of the OH stretching vibration band of water for different NaCl solutions from 0 to 300 °C at 30 MPa.

Figure 4. The relative RSCS of the OH stretching vibration band of water ($\sigma_{(m\text{NaCl}, T, 30 \text{ MPa})} / \sigma_{(\text{Pure water}, 20 \text{ }^\circ\text{C}, 30 \text{ MPa})}$) at 30 MPa as a function of temperature and NaCl concentration.

Figure 5. Comparison of the Raman spectra for different NaCl solutions at different temperatures.

Figure 6. Variations of the $\text{PAR}^*/m\text{CH}_4$ and the $\sigma_{(m\text{NaCl}, 20 \text{ }^\circ\text{C}, 30 \text{ MPa})} / \sigma_{(m\text{NaCl}, T, 30 \text{ MPa})}$ ratio as a function of temperature and NaCl concentration. The blank symbols represent $\text{PAR}^*/m\text{CH}_4$. The solid symbols are the $\sigma_{(m\text{NaCl}, 20 \text{ }^\circ\text{C}, 30 \text{ MPa})} / \sigma_{(m\text{NaCl}, T, 30 \text{ MPa})}$. The color of back, red and blue represent pure water, 3 m NaCl and 5 m NaCl aqueous system, respectively.

Table 1. The A , η and $\sigma_{(m\text{NaCl}, 20^\circ\text{C}, \text{Atm})}/\sigma_{(\text{Pure water}, 20^\circ\text{C}, \text{Atm})}$ for different NaCl solutions at 20 °C at atmospheric pressure

	A (Arbitr. Units)	η (mol/cm ³)	A/η	$\sigma_{(m\text{NaCl}, 20^\circ\text{C}, \text{Atm})}/\sigma_{(\text{Pure water}, 20^\circ\text{C}, \text{Atm})}$
Pure water	14500000	0.0555	261468028	1.000
1 m NaCl	14712500	0.0545	270070777	1.0329
2 m NaCl	14950000	0.0534	279788054	1.0701
3 m NaCl	15160000	0.0524	289506620	1.1072
5 m NaCl	15450000	0.0502	307532726	1.1762

Table 2 variation of the relative RSCS of the water OH stretching vibration band derived from experiment calculation and theoretical calculation.

T (°C)	$L_T/L_{20^\circ\text{C}}$	$S_T/S_{20^\circ\text{C}}$	$LS_T/LS_{20^\circ\text{C}}$	$\sigma_{(\text{Pure water}, T, 30 \text{ MPa})}/\sigma_{(\text{Pure water}, 20^\circ\text{C}, 30 \text{ MPa})}$
0	1.0015962	1.0000000	1.0015962	1.0331945
20	1.0000000	1.0000000	1.0000000	1.0000000
40	0.9968851	1.0000000	0.9968851	0.9749414
60	0.9927034	1.0000000	0.9927034	0.9465141
80	0.9876791	1.0000000	0.9876791	0.9247645
100	0.9819755	1.0000000	0.9819755	0.8959325
120	0.9756725	1.0000000	0.9756725	0.8760990
140	0.9688376	1.0000001	0.9688376	0.8369854
160	0.9614911	1.0000002	0.9614911	0.8251367
180	0.9536307	1.0000004	0.9536307	0.8029974
200	0.9452436	1.0000007	0.9452436	0.7816258
220	0.9362839	1.0000013	0.9362839	0.7530525
240	0.9266968	1.0000022	0.9266968	0.7306089
260	0.9163743	1.0000036	0.9163743	0.7223460
280	0.9051473	1.0000057	0.9051473	0.7025627
300	0.8927894	1.0000087	0.8927894	0.6803223

Figure 1

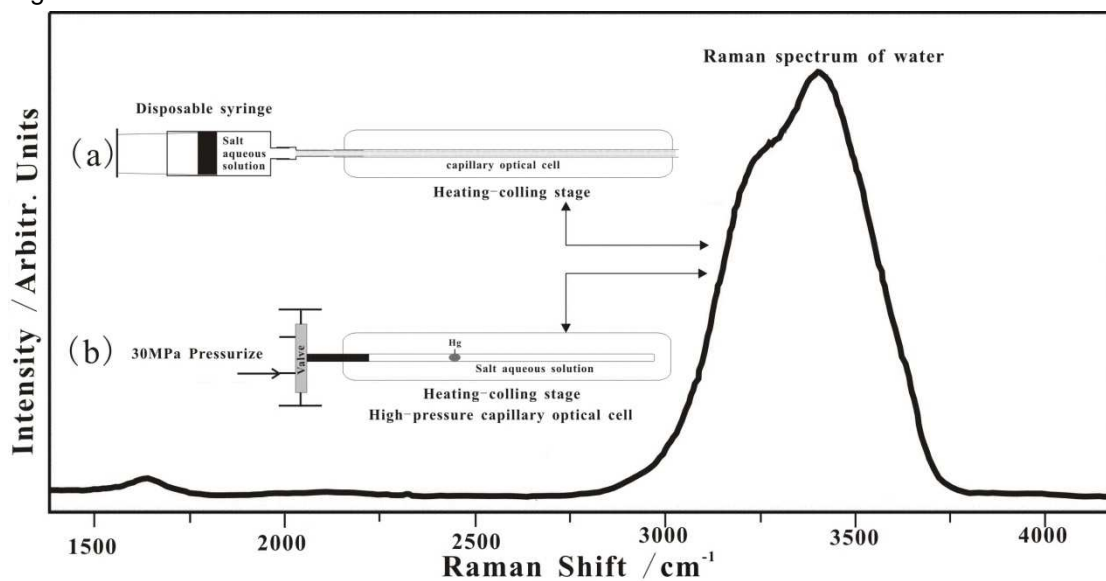


Figure 2

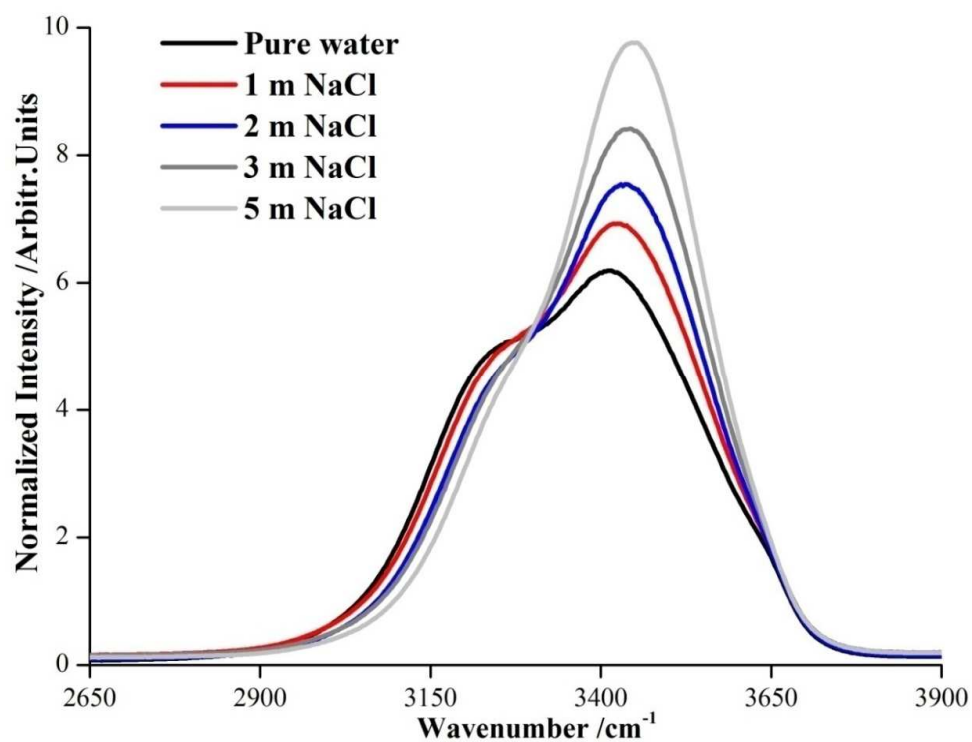


Figure 3

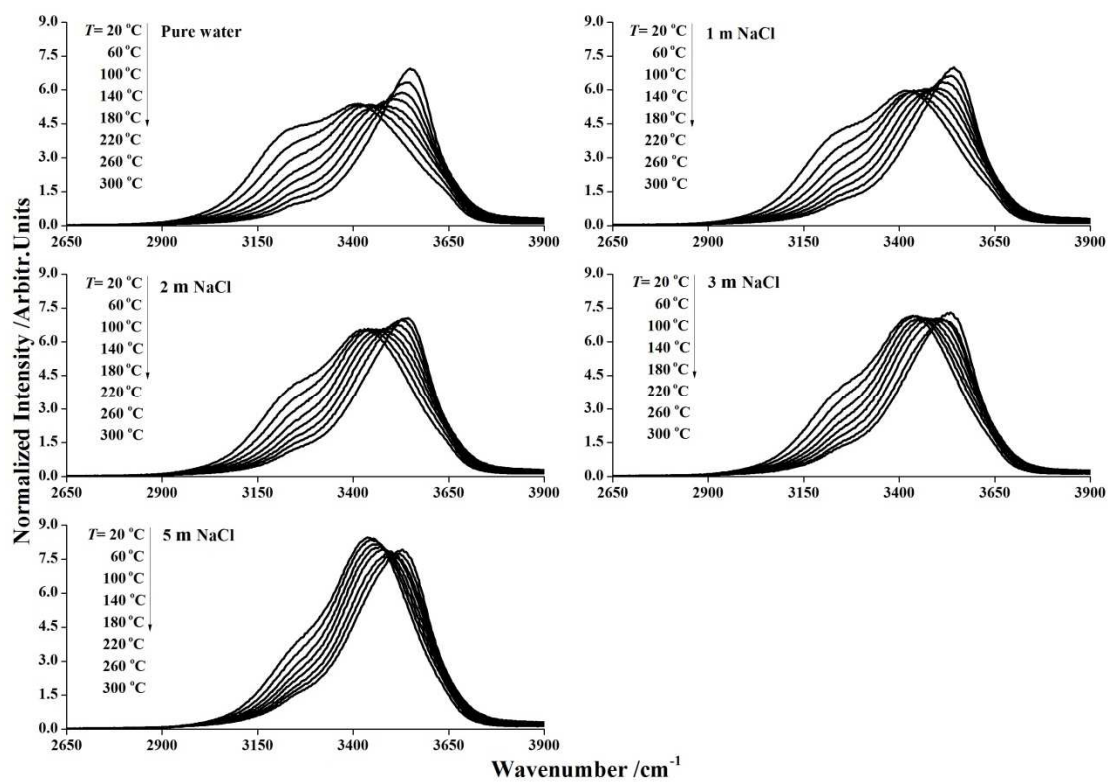


Figure 4

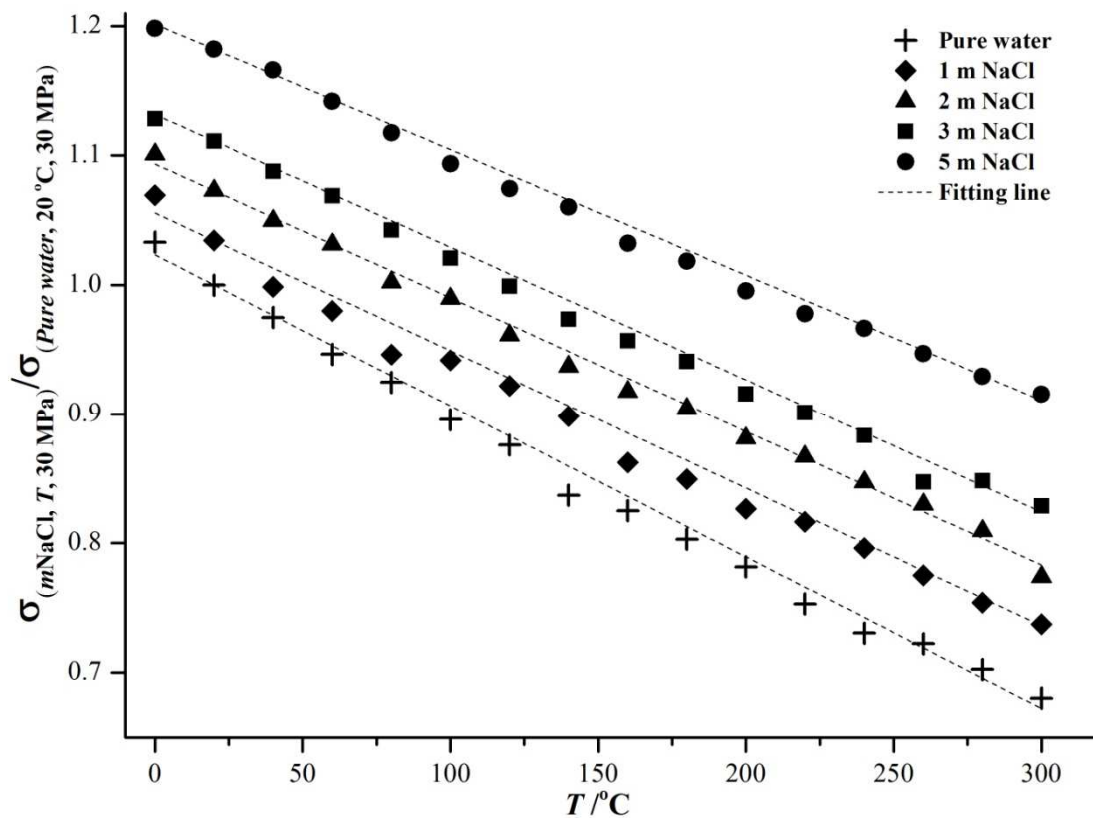


Figure 5

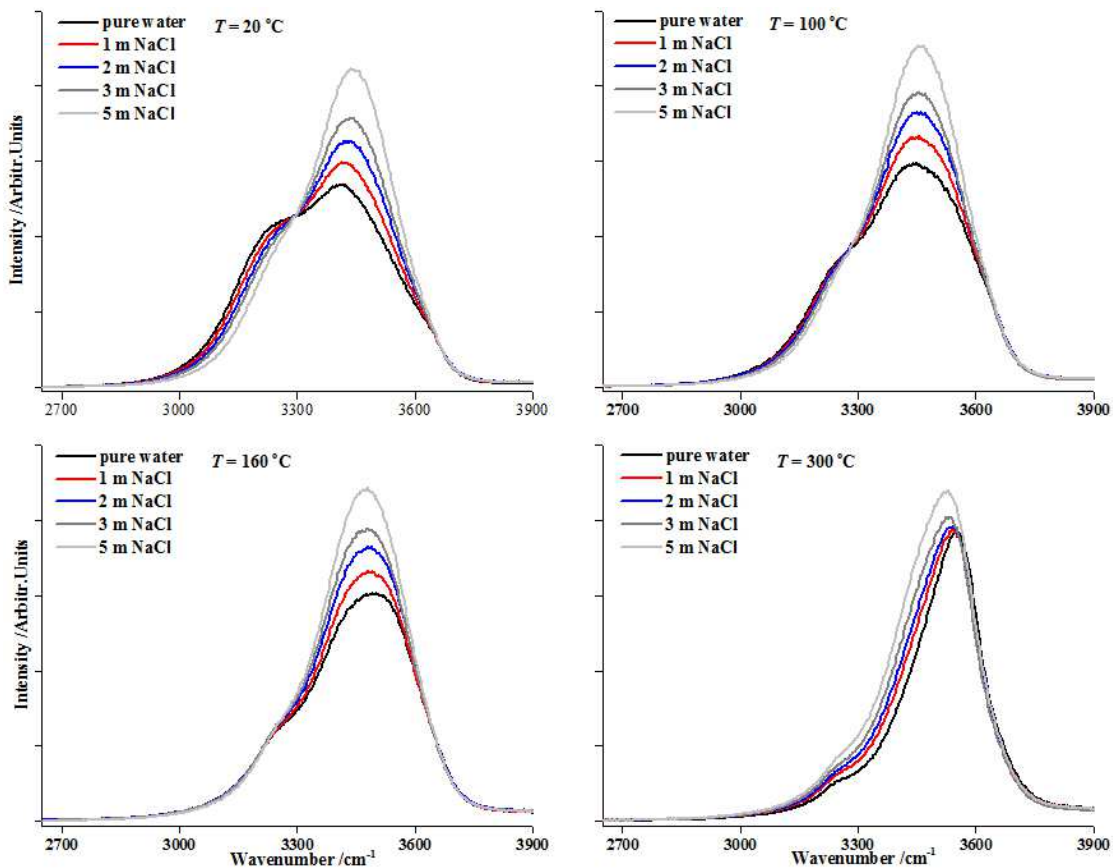


Figure 6

